

A Radio Survey for Linear and Circular Polarization in Low Luminosity Active Galactic Nuclei

Geoffrey C. Bower^{1,2}, Heino Falcke³ & Richard R. Mellon⁴

ABSTRACT

We conducted a Very Large Array survey of eleven low luminosity active galactic nuclei for linear and circular polarization at 8.4 GHz. We detected circular polarization in one source (M81*) and linear polarization in 3 sources. Sensitivity limits were $\sim 0.1\%$ for both modes of polarization in 9 of 11 sources. The detections confirm the importance of nonthermal emission in LLAGN. However, detection rates for circular and linear polarization are lower for these sources than for more powerful AGN. Fractional linear polarization in detected sources is also lower than in more powerful AGN. The weak linear polarization in the survey sources indicates their overall similarity to Sgr A*. Confusion with thermal sources, depolarization and weaker, less extended jets may contribute to these differences. We detect a rotation measure $\gtrsim 7 \times 10^4$ rad m⁻² for NGC 4579. This may arise from magnetized plasma in the accretion, outflow or interstellar regions. Inverted spectra are present in both M81* and Sagittarius A* and absent from all sources in which circular polarization is not detected. This suggests that optical depth effects are important in the creation of circular polarization.

Subject headings: galaxies: active — galaxies: individual (NGC 3031, NGC 3516, NGC 4278, NGC 4374, NGC 4486, NGC 4552, NGC 4579, NGC 4589, NGC 5216, NGC 6500, I 1024) — radio continuum: galaxies — polarization — radiation mechanisms: non-thermal — techniques: polarimetric

¹National Radio Astronomy Observatory, P.O. Box O, 1003 Lopezville, Socorro, NM 87801; gbower@nrao.edu

²Radio Astronomy Laboratory, University of California, Berkeley, CA 94720; gbower@astro.berkeley.edu

³Max Planck Institut für Radioastronomie, Auf dem Hügel 69, D 53121 Bonn Germany; hfalcke@mpifr-bonn.mpg.de

⁴Department of Astronomy and Astrophysics, Pennsylvania State University, University Park, PA 16803; rmellon@astro.psu.edu

1. Introduction

Circular and linear polarization are important diagnostics of nonthermal radio emission and its environment in extragalactic radio sources and galactic micro-quasars. In active galactic nuclei (AGN), linear polarization (LP) has been used to demonstrate that the emission mechanism is synchrotron radiation, that magnetic fields are present and that shocks propagate in jets, compressing the magnetic fields (e.g., Marscher & Gear 1985). LP is typically greater than 1% and is present in a very high fraction of powerful extragalactic radio sources (Aller et al. 1992). Rotation measures are used to study the plasma density and magnetic field in accretion and outflow regions of AGN (Taylor 2000).

The significance of circular polarization (CP) is less clear. A variety of mechanisms can produce the small levels of CP seen in these sources, including intrinsic and extrinsic origins (Jones & Odell 1977; Macquart & Melrose 2000; Broderick & Blandford 2000; Beckert & Falcke 2002; Ruszkowski & Begelman 2002). Synchrotron and cyclotron emission produce CP in varying degrees depending on the the electron population, magnetic field strength and orientation. Coherent emission processes may also lead to CP. In addition, the presence of electrons with Lorentz factors ~ 1 in or near a synchrotron source can significantly alter both CP and LP through Faraday effects. The combination of these effects can lead to complex polarized spectra. Finally, a magnetized scattering region can produce scintillating CP.

Recently, there has been a sharp increase in interest in CP observations. CP has been detected in Sagittarius A* (Bower et al. 1999b; Sault & Macquart 1999; Bower et al. 2002a), a large number of powerful extragalactic radio sources (Rayner et al. 2000; Homan et al. 2001) including some IDV sources (Macquart et al. 2000), and galactic microquasars (Fender et al. 2000, 2002). VLBI imaging of powerful extragalactic radio sources indicate that the CP is confined to the cores. The spectral and variability properties in these sources vary widely indicating potentially diverse origins. In most sources, LP dominates CP, as expected for simple synchrotron sources. A notable exception to this is Sgr A*, which exhibits no LP.

The polarization properties of low luminosity AGN (LLAGN) have not been previously investigated. Rudnick et al. (1986) observed the LP of a sample of “weak” radio sources ($L \sim 10^{23} - 10^{26} \text{ W Hz}^{-1}$) with flat spectra. Many of these sources were unpolarized at a level of 1% at 15 GHz, suggesting that they are not simply scaled down versions of powerful AGN. However, there exists a significant gap in luminosity between these sources and Sgr A*, which has a radio luminosity $\sim 10^{16} \text{ W Hz}^{-1}$.

The intrinsic nature of the LLAGN is still in doubt (for recent reviews see Ulvestad & Ho 2001; Nagar et al. 2002). These sources display emission line luminosities that may be produced through a variety of mechanisms, including stellar photoionization, collisional

ionization through shocks or in a starburst. A variety of methods have demonstrated that some of the sources display AGN-like characteristics. However, as in the case of Sgr A*, the luminosities are substantially sub-Eddington and there is dispute over the roles of advection, convection and outflow in these sources. The detection of high brightness temperature radio components has made a strong case for the role of jets in these sources. LP and CP can act as probes of the radio-emitting region as well as of the accretion and outflow regions through which the emission propagates.

We present here a radio polarization survey of 11 nearby LLAGN with luminosities in the range 10^{20} to 10^{23} W Hz⁻¹. In §2, we describe the observations, our error analysis and the results. CP is only detected in one source, NGC 3031 (M81*). We have discussed the significance of this detection in another paper (Brunthaler et al. 2001). LP is detected in 4 sources. We discuss our results in §3 and summarize in §4.

2. Observations

A sample of 11 LLAGN was selected from the samples of Wrobel & Heeschen (1991) and Ho et al. (1995). The selected sources (Table 1) are the brightest radio sources in the catalogs for which we were able to obtain data.

We observed the sample with the Very Large Array in the C configuration on 4 April 2000 for 12 hours at 8.4 GHz. The correlator was configured for continuum observations with 50 MHz bandwidth each in two intermediate frequency bands in right (RCP) and left circular polarization (LCP). The angular resolution was about 3".

Observations were carried out with the same techniques described in Bower et al. (1999b) and Bower et al. (2002a). Absolute flux calibration was set with a short observation of 3C 48. Scans of the target sources were bracketed with scans for pointing and calibration on a nearby background compact radio source. A second nearby background compact radio source was observed in the same way as the target sources as a check for CP calibration errors. We cycled through calibration and target sources in about 10 minutes. Calibrator, target and check sources were placed in five groups, labeled A through E, based on their proximity on the sky. Integration time for each target source was set to achieve rms noise errors of less than 0.1% except for the weak sources I 1024 and NGC 3516. Observations were made over 12 hours, leading to significant changes in parallactic angle, azimuth angle and elevation angle for each source. At least 4 observations were made of each source.

Data were reduced in AIPS. The calibration sources were self-calibrated assuming $V = 0$. Linear polarization calibration was also performed using the calibration sources. Amplitude

gains, phase gains and polarization leakage terms were transferred to the target and check sources. All sources were imaged in Stokes I, Q, U and V. Flux densities were estimated by fitting Gaussians at the source’s location. Results are summarized in Table 1. Some sources were resolved in total intensity. However, polarization images were unresolved for all sources except NGC 4374 and NGC 4486. We plot the linear and circular polarizations together in Figure 1.

Systematic errors from beam squint, gain and leakage terms are estimated according to the model for the VLA in Bower et al. (2002a) to be between 0.03 and 0.05% in total, depending on the number of scans per source. We see that that measured CP for the check sources range from 0.03 to 0.45% with a median of 0.14%. The likely source of additional error is polarization of the calibrator and/or check source. NGC 3031 is the only source where the measured CP exceeds that of the check source and is greater than 3 times the thermal noise. The CP for NGC 3031 is, in fact, 10 times the thermal noise and repeatedly detectable (Brunthaler et al. 2001). We do not count NGC 6500 as a CP detection because of the large measured CP for the check source, J1745+173. The two large CP values with the same sign suggest that the calibrator, J1751+096, may have CP at a level of $\sim -0.4\%$. Homan & Wardle (1999) report a tentative detection of $\sim -0.1\%$ for J1751+096 in their 15 GHz VLBA observations, which is consistent in sign and in magnitude for a steep spectral index.

3. Discussion

3.1. Confusion

For all sources, the measured polarization fractions are lower limits to the polarization of the nuclear source. For a typical distance of 10 Mpc, the linear resolution of these observations is ~ 100 pc. Diffuse thermal radiation can contribute significantly to the total flux. However, for the sources for which we know of VLBI observations, the compact radio flux is a substantial component of the total flux. NGC 3031 and NGC 4486 (M87) both have well-studied VLBI properties, which show that a compact core dominates the total flux (Junor et al. 1999; Bietenholz et al. 2000). Falcke et al. (2000) and Nagar et al. (2001) also show that the ratio of 5 GHz VLBA to VLA flux densities is on the order of unity for five of our sources: NGC 4278, NGC 4374, NGC 4552, NGC 4579 and NGC 6500. For all 13 sources in the Nagar et al. (2001) sample, the ratio is greater than 0.48. Nevertheless, a factor of a few in the ratio of total to compact flux density would raise the polarization limits to the point where Sgr A* and NGC 3031 would not be detected.

3.2. Linear Polarization

We detect LP in 3 of 11 sources: NGC 4278, NGC 4486, and NGC 4579. These results show that some LLAGN do exhibit LP, contrary to the conclusions of Rudnick et al. (1986), which were based on less sensitive data. This is strong evidence for a nonthermal contribution to the flux density.

However, the rate of detection of LP is lower than that of more powerful AGN. For example, Homan et al. (2001) detect LP in all but 3 of their 40 sources with a mean value of a few percent. In addition, the fraction of LP detected in our sources is lower than in more powerful AGN. Excluding M87, the mean fractional LP is $\sim 0.2\%$. Of the 62 sources in the Pearson-Readhead flux-limited sample, 39 have polarization greater than 1% at 4.8 GHz and 57 have polarization greater than 1% at 15 GHz (Aller et al. 1992). Mean polarizations are on the order of a few percent. These trends are true for quasars, BL Lac objects and radio galaxies in the sample. This difference cannot be explained by confusion. All three sources have been previously detected with VLBI and been shown to be dominated by their compact flux (Junor et al. 1999; Nagar et al. 2001).

Are the LLAGN intrinsically weakly polarized or are they depolarized by their surrounding medium? A number of scenarios may lead to intrinsic depolarization. Extreme magnetic field disorder in the source will leave the source weakly polarized. This may be due to the absence of shocks in jets that order the field and produce regions of high polarization fraction. A high degree of symmetry in the magnetic field, i.e., a face on azimuthal field or a radial field will also lead to a weakly polarized source. Such field configurations might be typical of disk accretion or quasi-spherical accretion. Finally, internal Faraday depolarization may occur if the density of nonrelativistic particles in the emitting region is large enough (e.g., Beckert & Falcke 2002; Ruszkowski & Begelman 2002).

On the other hand, depolarization in the accretion, outflow or surrounding regions is more than adequate to account for this result. Beam and bandwidth depolarization at these frequencies and in these bandwidths will occur for rotation measures of 10^3 rad m^{-2} and 10^5 rad m^{-2} , respectively. Taylor (2000) has measured RMs as large as $2 \times 10^3 \text{ rad m}^{-2}$ towards the cores of powerful AGN. Bower et al. (2002b) have measured a $\text{RM} \sim 4 \times 10^5 \text{ rad m}^{-2}$ towards Sagittarius A*, which may arise from the accretion and outflow regions or from an interstellar halo. Even for the very low accretion rates of ADAF and CDAF models of Sgr A*, RMs can easily reach 10^6 rad m^{-2} and higher (Bower et al. 1999a; Quataert & Gruzinov 2000). The radio emission from our sources almost certainly propagates through similar media. In the case of NGC 4258, for example, the radio emission originates from within 0.02 pc of the black hole (Herrnstein et al. 1998). On the other hand, the radio emission from much more powerful AGN may begin parsecs away from the black hole.

The radio intermediate quasar III Zw 2 provides an interesting case for comparison. This compact radio source (< 1 pc) shows superluminal expansion and spectral evolution consistent with shock excitation in a relativistic outflow (Brunthaler et al. 2001). However, the source exhibits no linear polarization in 20 years of monitoring (M. Aller, private communication).

In order to look for the effects of bandwidth depolarization and large RMs, we compared the difference between lower and upper sideband position angles for all sources. These sidebands are each 50 MHz wide and separated from each other by 50 MHz. We find a significant change only for NGC 4579 of 60 ± 13 degrees. Systematic error due to leakage term miscalibration is less than 10 degrees. By comparison, NGC 4278, which is polarized at a level similar to NGC 4579, shows a difference of 6 degrees in the position angle. Changes in the position angle for calibrator sources were also consistent with thermal noise. The implied RM for NGC 4579 is $\sim 7 \times 10^4$ rad m⁻². This would lead to bandwidth depolarization ~ 0.5 , which does not significantly increase the intrinsic LP. However, one cannot rule out a much higher RM inducing more substantial depolarization as well as the angular rotation. We can compute an upper limit for the RM $\sim 10^7$ rad m⁻² with the requirement of a maximum of 70% intrinsic polarization.

As discussed above, this RM could arise from a variety of sources. Without more detailed knowledge of the source geometry, it is difficult to place limits on specific source models such as jet, ADAF and CDAF models. Unlike the case of millimeter wavelength polarization in Sgr A*, the centimeter wavelength emission from NGC 4579 may originate far outside of the accretion region. However, if the emission does pass through the accretion region, then the accretion rate must be very low (Bower et al. 1999a; Quataert & Gruzinov 2000).

Spectropolarimetry, higher frequency polarimetry and VLBI polarimetry are potentially useful tests of these scenarios. They could provide quantitative information about field strengths and particle densities in the inner few parsecs of these sources.

3.3. Circular Polarization

We compare the rates of detection of CP here with that in powerful extragalactic radio sources. At a level of $\sim 0.1\%$, we detect 1 out of 9 sources. Rayner et al. (2000) detect CP greater than 0.1% in 12 out of 30 sources. Homan et al. (2001) detect CP greater than 0.1% in 11 out of 40 sources. Due to the small number of sources in our sample, we cannot conclude that the rate of CP in LLAGN is less than that in powerful AGN. However, the trend appears to be that way.

What physical condition leads to the presence of CP in some sources and not in others? NGC 3031 and Sgr A* are both unique in that they have inverted spectra at the frequencies where CP is detected. We summarize the spectral index information for sources where simultaneous spectra are available in Figure 1. All spectral indices come from the measurements of Nagar et al. (2001). While the number of sources is small, the trend is apparent.

This effect may be the result of an inhomogeneous synchrotron source in the optically thick regime (Beckert & Falcke 2002; Ruszkowski & Begelman 2002). Orientation effects may also be of importance since the magnitude of CP from a synchrotron source depends on the line of sight magnetic field strength. Finally, NGC 3031 is also the closest of our survey sources, suggesting that resolution of thermal sources in the nucleus and of extended optically, thin regions in the jet may be important.

4. Conclusions

We have observed linear and circular polarization in a sample of low luminosity AGN. The polarization properties of these sources differ from those of more powerful AGN. Linear polarization is less frequently detected and less strong when detected. Circular polarization is less frequently detected. The conclusion is not as simple as claiming that these sources differ intrinsically from the more powerful AGN, however. While increased field disorder in the sources could explain the results, environmental depolarization effects could also play a role.

These polarization measurements probe regions on a scale of parsecs and smaller in these sources. Detection of rotation measures in these sources is a direct measure of the environment of a supermassive black hole, which may be used to constrain models for accretion and outflow.

A broader sample of sources is necessary to demonstrate that the trends we see are statistically significant. VLBI polarimetric imaging and spectropolarimetry may also test some of these conclusions.

The National Radio Astronomy Observatory is a facility of the National Science Foundation operated under cooperative agreement by Associated Universities, Inc. This research has made use of data from the University of Michigan Radio Astronomy Observatory which is supported by funds from the University of Michigan.

REFERENCES

- Aller, M. F., Aller, H. D., & Hughes, P. A. 1992, *ApJ*, 399, 16
- Beckert, T. & Falcke, H. 2002, *A&A*, 388, 1106
- Bietenholz, M. F., Bartel, N., & Rupen, M. P. 2000, *ApJ*, 532, 895
- Bower, G. C., Backer, D. C., Zhao, J. H., Goss, M., & Falcke, H. 1999a, *ApJ*, 521, 582
- Bower, G. C., Falcke, H., & Backer, D. C. 1999b, *ApJ*, 523, L29
- Bower, G. C., Falcke, H., Sault, R. J., & Backer, D. C. 2002a, *ApJ*, 571, 843
- Bower, G. C., Wright, M. C. H., Falcke, H., & Backer, D. C. 2002b, *ApJ* submitted
- Broderick, A. & Blandford, R. D. 2000, *BAAS*, 197, #83.15
- Brunthaler, A., Bower, G. C., Falcke, H., & Mellon, R. R. 2001, *ApJ*, 560, L123
- Falcke, H., Nagar, N. M., Wilson, A. S., & Ulvestad, J. S. 2000, *ApJ*, 542, 197
- Fender, R., Rayner, D., McCormick, D., Muxlow, T., Pooley, G., Sault, R., & Spencer, R. 2002, *MNRAS* in press
- Fender, R., Rayner, D., Norris, R., Sault, R. J., & Pooley, G. 2000, *ApJ*, 530, L29
- Herrnstein, J. R., Greenhill, L. J., Moran, J. M., Diamond, P. J., Inoue, M., Nakai, N., & Miyoshi, M. 1998, *ApJ*, 497, L69
- Ho, L. C., Filippenko, A. V., & Sargent, W. L. 1995, *ApJS*, 98, 477
- Homan, D. C., Attridge, J. M., & Wardle, J. F. C. 2001, *ApJ*, 556, 113
- Homan, D. C. & Wardle, J. F. C. 1999, *AJ*, 118, 1942
- Jones, T. W. & Odell, S. L. 1977, *ApJ*, 214, 522
- Junor, W., Biretta, J. A., & Livio, M. 1999, *Nature*, 401, 891
- Macquart, J. P., Kedziora-Chudczer, L., Rayner, D. P., & Jauncey, D. L. 2000, *ApJ*, 538, 623
- Macquart, J. P. & Melrose, D. B. 2000, *ApJ*, 545, 798
- Marscher, A. P. & Gear, W. K. 1985, *ApJ*, 298, 114

Nagar, N. M., Falcke, H., Wilson, A. S., & Ulvestad, J. 2002, A&A in press

Nagar, N. M., Wilson, A. S., & Falcke, H. 2001, ApJ, 559, L87

Quataert, E. & Gruzinov, A. 2000, ApJ, 545, 842

Rayner, D. P., Norris, R. P., & Sault, R. J. 2000, MNRAS, 319, 484

Rudnick, L., Jones, T. W., & Fiedler, R. 1986, AJ, 91, 1011

Ruszkowski, M. & Begelman, M. C. 2002, ApJ, 573, 485

Sault, R. J. & Macquart, J.-P. 1999, ApJ, 526, L85

Taylor, G. B. 2000, ApJ, 533, 95

Ulvestad, J. S. & Ho, L. C. 2001, ApJ, 562, L133

Wrobel, J. M. & Heeschen, D. S. 1991, AJ, 101, 148

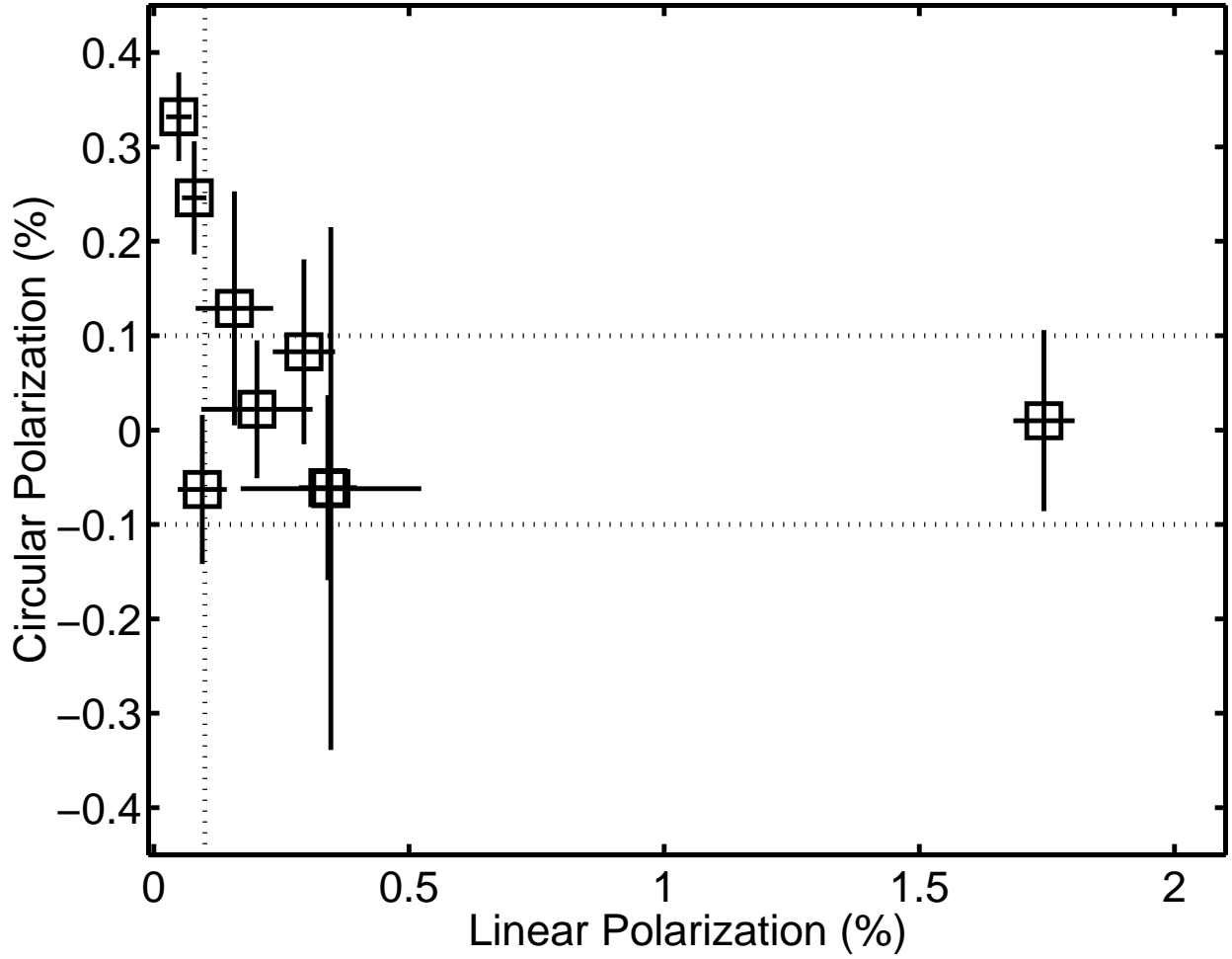


Fig. 1.— Linear and circular polarization for the survey sources. Plotted error bars are $1 - \sigma$ thermal errors. Dotted lines indicate the characteristic systematic errors in linear and circular polarization of 0.1%. We have excluded non-detections for I 1024 and NGC 3516 due to the substantially larger fractional errors for these sources.

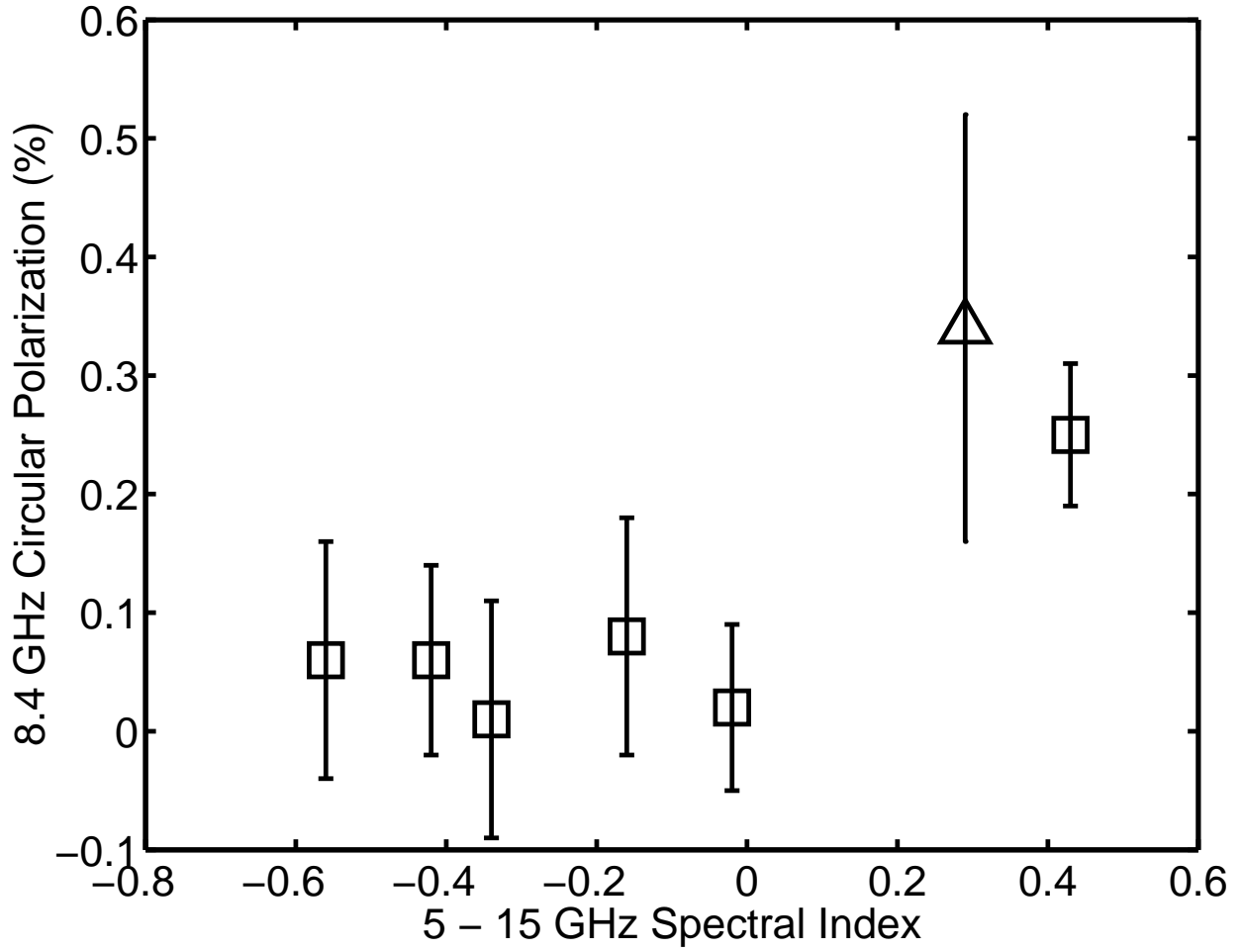


Fig. 2.— Absolute value of circular polarization at 8.4 GHz as a function of spectral index between 5 and 15 GHz. Squares are for sources in the sample for which 5 to 15 GHz contemporaneous flux density measurements are available. The triangle is for Sgr A*.

Table 1. Polarized and Total Flux from VLA Continuum Observations at 8.4 GHz

Group	Source	Source Type	$I \pm \sigma$ (mJy)	$V \pm \sigma$ (%)	$P \pm \sigma$ (%)	$\chi \pm \sigma$ deg	Resolved (Y/N)
A	1048+717	calibrator	1541.6 ± 0.2	-0.00 ± 0.01	0.89 ± 0.00	-21.0 ± 0.2	N
A	1056+701	check source	467.5 ± 0.6	0.14 ± 0.03	1.76 ± 0.01	81.5 ± 0.3	N
A	NGC 3031	SrBI-II	263.1 ± 0.5	0.25 ± 0.06	0.08 ± 0.02	-29.8 ± 6.1	N
A	NGC 3516	RSBO ₂	2.9 ± 0.0	-0.76 ± 1.25	0.83 ± 0.59	-13.3 ± 23.1	Y
A	NGC 4589	E2	13.0 ± 0.0	-0.06 ± 0.28	0.35 ± 0.18	-10.5 ± 14.2	N
B	1400+621	calibrator	1140.8 ± 0.2	-0.00 ± 0.01	0.15 ± 0.01	23.1 ± 1.1	N
B	1335+587	check source	671.5 ± 1.9	0.16 ± 0.04	0.13 ± 0.01	36.3 ± 1.3	N
B	NGC 5216	E/S0	37.9 ± 0.1	0.13 ± 0.12	0.16 ± 0.08	76.0 ± 6.9	N
C	1158+248	calibrator	555.7 ± 0.1	0.01 ± 0.02	0.12 ± 0.01	-15.0 ± 2.7	N
C	1221+282	check source	732.9 ± 1.2	0.03 ± 0.04	5.54 ± 0.02	5.8 ± 0.1	N
C	NGC 4278	E1	76.5 ± 0.3	-0.06 ± 0.10	0.34 ± 0.06	15.7 ± 7.0	N
C	1239+075	check source	580.4 ± 1.8	-0.07 ± 0.03	5.26 ± 0.02	-56.6 ± 0.1	N
C	NGC 4374	E1	183.4 ± 2.4	0.02 ± 0.07	0.20 ± 0.11	14.8 ± 22.3	Y
C	NGC 4486	E0	3351.3 ± 30.9	0.01 ± 0.10	1.74 ± 0.06	22.0 ± 1.5	Y
C	NGC 4552	SO ₁	94.1 ± 0.2	-0.06 ± 0.08	0.09 ± 0.05	-39.5 ± 15.5	N
C	NGC 4579	SabII	45.9 ± 0.1	0.08 ± 0.10	0.29 ± 0.06	-32.0 ± 9.0	N
D	1430+107	calibrator	908.2 ± 0.2	0.00 ± 0.01	0.04 ± 0.00	0.1 ± 5.1	N
D	1445+099	check source	604.9 ± 0.8	0.24 ± 0.03	1.04 ± 0.01	66.6 ± 0.4	N
D	I 1024	S0	1.4 ± 0.0	-1.53 ± 1.60	1.96 ± 1.02	30.1 ± 20.9	Y
E	1751+096	calibrator	2498.2 ± 0.3	-0.00 ± 0.01	8.33 ± 0.00	-25.5 ± 0.0	N
E	1745+173	check source	797.4 ± 0.9	0.45 ± 0.03	2.87 ± 0.01	58.2 ± 0.1	N
E	NGC 6500	Sbc	138.6 ± 0.2	0.33 ± 0.05	0.05 ± 0.03	-33.2 ± 9.3	N